ARTICLE

A new cucurbit[10]uril-based AIE fluorescent supramolecular polymer for cellular imaging

Received 00th January 20xx,
Accepted 00th January 20xx

DOI: 10.1039/x0xx00000x

Yang Luo[1‡], Shiquan Gan[2‡], Wei Zhang[1], Menghao Jia[2], Lixia Chen[1], Carl Redshaw [3], Zhu Tao[1], Xin Xiao[1*]

To further advance the development of cucurbit[10]uril-based supramolecular biomaterials, an AIE fluorescent supramolecular polymer (TPE-B@Q[10]) was constructed from the newly synthesized AIE molecule TPE-B and Q[10] via host-guest interactions in a host/guest ratio of 1:2. TPE-B@Q[10] not only has excellent blue fluorescence emission properties, but also possesses good biocompatibility and low toxicity. Therefore, TPE-B@Q[10] was successfully used for cytoplasmic imaging of cells. Flow cytometry further illustrated that Q[10] is capable of generating an alternative way to increase the fluorescence of TPE-B and its characteristic pattern for cellular imaging. This work provides a theoretical basis for promoting the application of cucurbit[*n*]uril-based supramolecular polymers in cell biology, and promotes the further development of cucurbit[*n*]uril chemistry.

Introduction

In 1987, Lehn and co-workers reported that supramolecular polymers with liquid crystal properties can be assembled by utilizing triple hydrogen bonding, the field of supramolecular polymers has rapidly developed and now impacts several other areas [1-4]. The formation of supramolecular polymers is driven mainly by non-covalent bonds, such as multiple hydrogen bonds, π-π interactions, metal coordination bonds, and host-guest interactions [5-8]. Among these, host-guest interactions are the commonest force typically utilized by supramolecular polymers. Cucurbit[*n*]urils (Q[*n*]s, n=5-8,10,13-15) are classic macrocyclic compounds possessing a rigid hydrophobic cavity, and impart unique characteristics on the construction of supramolecular polymers due to their high binding constants with a variety of guest molecules [9-15]. Indeed, there are now many examples involving the use of cucurbit[*n*]uril and their unique cavities to construct supramolecular polymers [16-18], and such systems make full advantage of both the Q[*n*]'s rigid hydrophobic cavity and its unique host-guest chemistry. Such work reveals how Q[*n*]s are an excellent building block for connecting organic molecular components to construct supramolecular polymers. Q[*n*]-based supramolecular biomaterials have attracted great attention in recent years [19-21]. Q[10], as the largest cavity Q[*n*], not only has the traditional rigid cavity but also has the powerful ability to accommodate multiple molecules unmatched by other Q[*n*]s, but has been slow to be studied in biomaterials especially in bioimaging research [22-26]. Therefore, this paper selects the well-known TPE molecular derivative as the guest molecule and tries to explore the potential value and superiority of Q[10] in the study of biomaterials.

The tetraphenylethenes (TPE) are a simple but classic aggregation-induced emission (AIE) family of compounds first discovered by Tang *et al*. [27]. They possess such characteristics as a unique structure with four rotating "arms", as well as strong fluorescence after aggregation, which can be used in systems for biological detection [28-30]. These attributes make them an excellent choice for constructing 2D cross-linked supramolecular polymers [31,32], and particularly for the construction of supramolecular polymers based on TPE and Q[*n*]s [33-35]. For example, a light-tunable 2D SOF (supramolecular organic framework) based on TPE-4MV, Q[8], and an azobenzene derivative has been constructed in aqueous solutions through host-guest interactions, which can be dissociated under UV light. Tang and coworkers also recently utilized TPE derivatives and Q[8] to construct supramolecular polymers and successfully applied them to cell classification [33].

1. *Key Laboratory of Macrocyclic and Supramolecular Chemistry of Guizhou Province, Guizhou University, Guiyang 550025, China.*
2. *State Key Laboratory of Functions and Applications of Medicinal Plants, School of Pharmaceutical Sciences, Guizhou Medical University, Guiyang 550014, China*
3. *Department of Chemistry, University of Hull, Hull HU6 7RX, U.K*

‡ Joint first authors
** Corresponding author: gyhxxiaoxin@163.com*

Given the above, we have synthesized a new water-soluble TPE derivative, namely TPE-B (Scheme 1 for the structure and Scheme S1 for the synthesis) to be used as a guest, while the less researched molecule Q[10] (Figure 1) is selected as the host [11,12,36-38]. As expected, the huge cavity of the Q[10] simultaneously encompasses the arms of two TPE-B through host-guest interactions to construct a 2D cross-linked supramolecular AIE polymer (TPE-B@Q[10]), which exhibits a good fluorescence performance. In addition, TPE-B@Q[10] was found to have not only good cytocompatibility, low biotoxicity, but most importantly, very good fluorescence imaging in the cytoplasm of cells, which provides a good basis for subsequent studies on organelle localization, Q[10] loading of third drug guest molecules for in vivo tracking, *etc.*

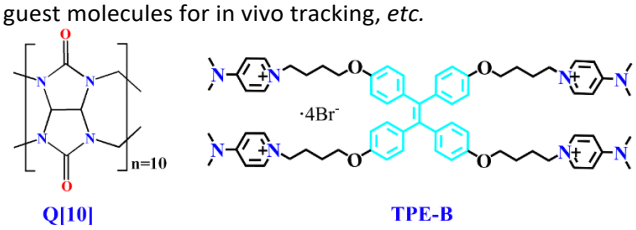

Scheme 1. The chemical structures of Q[10] and TPE-B.

Results and discussion

The supramolecular self-assemble behavior between TPE-B and Q[10] was first investigated by fluorescence spectroscopy (Figure 1). The unbounded TPE-B emits faint blue emission at 485 nm under excitation at 339 nm due to the constantly rotating "arm". Interestingly, the fluorescence intensity of the AIE compound TPE-B is substantially increasing with the addition of Q[10] from 327 a. u. up to 985 a. u., *i.e.* increased about 3-fold. The root cause of the increase in the FL intensity is that the intramolecular rotation of the TPE-B becomes restricted by the presence of additional Q[10]. The increased amount of Q[10] forces the rotating phenyl rings of TPE-B to turn into the aromatic planes, which effectively inhibits the non-radiative annihilation process of the AIE compound TPE-B, and thus TPE-B can emit a stronger blue fluorescence. In addition, an obvious fluorescence enhancement can be observed with the naked eye (insert of Figure 1a). Under the excitation of a 365 nm UV lamp, it can be seen that the solution of TPE-B in the presence of Q[10] emits stronger fluorescence, while the fluorescence of free TPE-B is very weak. At the same time, an obvious blue shift from λ_{em} = 485 nm to 433 nm ($\Delta\lambda_{em}$ = 52 nm) in fluorescence emission wavelength can be observed. The reason for this phenomenon is mainly due to the change in the micro-environment of the TPE-B after it enters the hydrophobic cavity of the Q[10]. In other words, TPE-B responds to the low-polarity cavity of Q[10] after binding with it. Strong aggregation of TPE-B@Q[10] can also be seen from the confocal fluorescence microscopy images (Figure 1c and d). Moreover, the molar ratio of TPE-B@Q[10] is calculated as Q[10]:TPE-B = 2:1, which is consistent with Job's plot (Figure 1b).

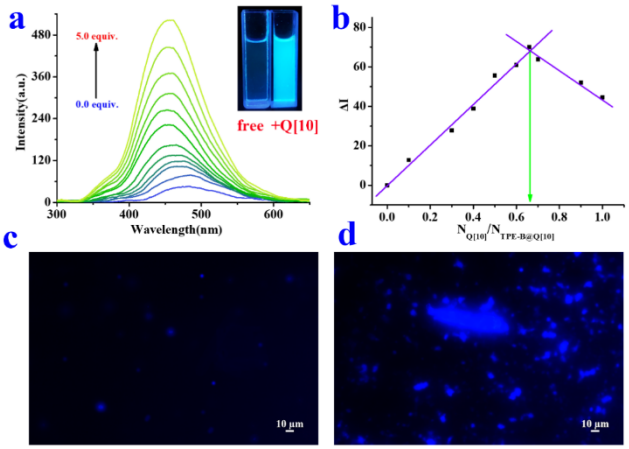

Figure 1 Fluorescence spectra (a) of TPE-B (20 μM) upon addition of Q[10] with λex=339 nm (the TPE-B/Q[10] molar ratio changed from 1:0 to 1:5). Job's plot (b) of Q[10] and TPE-B and the confocal microscopy images of 5 mM TPE-B (c) and 5 mM TPE-B@Q[10] (d).

^{1}H NMR spectroscopy can be used to further explore the interaction, and as shown in Figure 2, the characteristic signal peak of Q[10] shifts to lower field (from δ = 5.61 to 5.66 ppm, δ = 5.31 to 5.36 ppm, δ = 3.99 to 4.05 ppm) due to the micro-environment change of the cavity. At the same time, all the proton signals associated with TPE-B shifts significantly to high field upon addition of Q[10] (from δ_c = 7.77 to 7.31ppm, δ_h = 6.78 to 6.24ppm, δ_h = 6.65 to 6.17ppm, δ_i = 6.53 to 6.09ppm, δ_d = 3.81 to 3.66ppm, δ_a = 2.98 to 2.75ppm, δ_e = 1.80 to 1.39ppm, δ_f = 1.51 to 1.05ppm). Therefore, it can be concluded that Q[10] binds the entire alkyl chain and the 4-dimethylaminopyridine group of TPE-B in a molar ratio of $N_{Q[10]}$: N_{TPE-B} = 2:1. The above characterization can be interpreted by the preliminary formation of a networked AIE supramolecular complex (TPE-B@Q[10]).

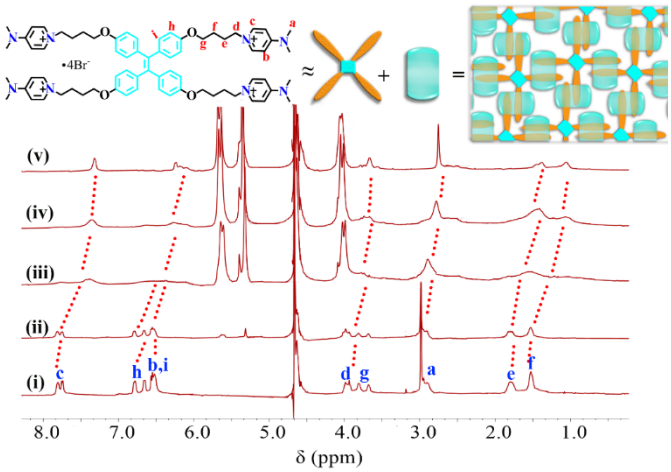

Figure 2. ^{1}H NMR spectra of TPE-B (5 mM) with increasing amounts of Q[10] from 0.0, 0.5, 1.0, 1.5, and 2 recorded in D_2O at 25 ℃.

Next, isothermal titration calorimetry (ITC) was applied to the thermodynamic analysis of the formation of TPE-B@Q[10]. Using the Multiple Sites model to simulate a series of ITC data (Figure S8 and Table S1), it was found that when two molar equivalents of Q[10] enclose one molar equivalent of TPE-B, the ΔG_2 (-17.1KJ/mol) of their interaction is negative. This indicates

that the formation of the supramolecular polymer TPE-B@Q[10] can proceed spontaneously and that the elevation of temperature promotes its formation. Meanwhile, the corresponding K_a is calculated as 2.77×10^8 M^{-2} indicating that the TPE-B@Q[10] also has a high binding ability.

The morphology of TPE-B@Q[10] was further verified by the use of scanning electron microscopy, and a somewhat loose and porous structure could be observed. In addition, both DLS and DOSY have also provided further supporting data, among which the hydrodynamic diameter (D_h) of the supramolecular polymer increases significantly from 98.732 nm to 312.452 nm, and the diffusion coefficient of the supramolecular polymer significantly reduced from 3.599×10^{-10} m^2s to 2.187×10^{-10} m^2s.

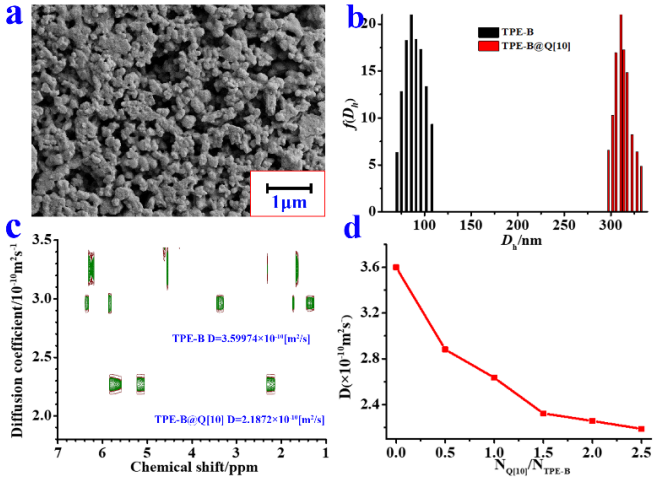

Figure 3. The SEM (a) of TPE-B@Q[10]; DLS (b) of TPE-B (1 mM) and TPE-B@Q[10] (1 mM); DOSY (c, d) of TPE-B (1 mM) towards Q[10].

The supramolecular polymer TPE-B@Q[10] cleverly solves the weak luminescence problem of TPE-B at low concentrations, which means it can perform better in biological detection applications, such as cell imaging. Cytotoxicity experiments have shown that TPE-B@Q[10] does not influence the viability and morphology of Hela and HUVEC cells, satisfying the basic experimental conditions for live cell imaging (Figure S11). As shown in Figure 4, TPE-B was added to the media of HUVEC and HeLa cells. Once entering the cytoplasm, TPE-B can exert the weak fluorescence under microscopy but was hard to observe. Extra Q[10] was added to the TPE-B in the molar ratio 2:1, and this remarkably enhanced the total fluorescence intensity in spite similar number of cells being counted in the field of view of the microscope, suggesting the ability of Q[10] to enhance TPE-B fluorescence and its capability to produce cell images. The fluorescent images could not be detected until the concentration of TPE-B in the media is greater than 2 μM, so we incubated HUVEC and Hela cells with TPE-B at a final concentration of 2 μM to optimize the fluorescence genesis condition. The fluorescent signal in both the A channel and B channel is increased significantly once surplus Q[10] is added into the media compared with TPE-B staining alone. It is worth emphasizing that the addition of Q[10] enhances the fluorescence signal of TPE-B in a relatively short time (becoming evident in less than 5 minutes and stable for more than 30 minutes), making it a quick and simple staining material for identifying different kinds of cells. Meanwhile, the application of the TPE-B complex needs no equipment upgrade for the excitation and emission wavelength of TPE-B@Q[10] happens to meet the normal parameter of DAPI (λ_{ex} = 364 nm, λ_{em} = 454 nm. Therefore, it provides the possibility of applying TPE derivatives in cell imaging while eliminating the shortcomings of using TPE alone.

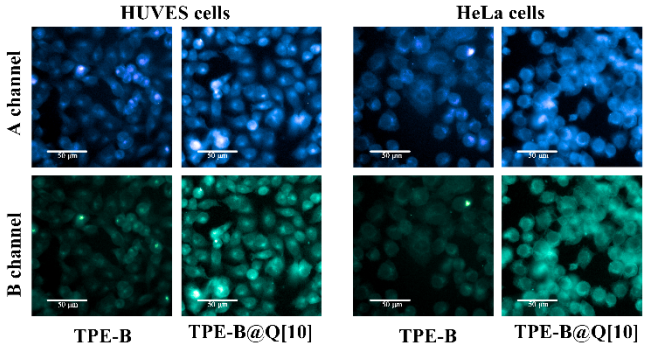

Figure 4. High Content Analysis System images of HUVEC cells (normal) and Hela cells (cancer) co-stained with TPE-B (2 μM) and TPE-B@Q[10] (2 μM) at 37 ℃. A channel: λ_{ex} = 355-385 nm, λ_{em} =430-500 nm; B channel: λ_{ex} = 355-385 nm, λ_{em} =470-515 nm. The scale for each image is 50 μm.

Another interesting result was that Q[10] not only promoted the fluorescence intensity of TPE-B in these two sets of cells, but also produced an emission light shift from 485 nm to 430 nm. To prove this phenomenon, a combination of TPE-B and Q[10] (in the molar ratio of 1:2) was put into the media of HeLa and HUVEC cells, then the cell fluorescence was captured with a 488 nm emission filter of cytometry. In Figure 5, it also can be seen that there is a shift from the fluorescence peak of TPE-B to the fluorescence peak of TPE-B@Q[10], implying that the fluorescence intensity of the TPE-B at 488 nm in the HeLa and HUVEC cells was profoundly reduced when Q[10] was added despite the continuous accumulation of the TPE-B fluorescence signal in both the TPE-B and TPE-B@Q[10] groups. This illustrated that Q[10] interrupted the emission spectrum of TPE-B, thus generating an alternative way to increase the fluorescence of TPE-B and improve the characteristic pattern for cellular imaging.

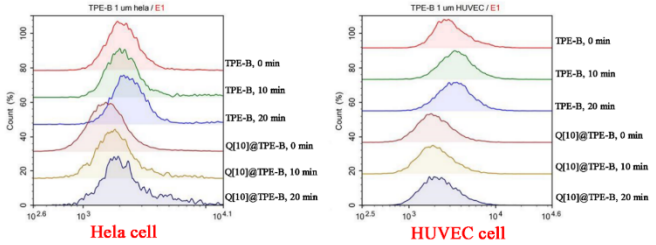

Figure 5. Statistical analysis of HUVEC cells (normal) and Hela cells (cancer) stained by TPE-B (1 μM) and TPE-B@Q[10] (1 μM), respectively, at different time points by flow cytometry. λex = 405 nm, λem = 488 nm. Q[10] promoted the shift of the emission spectrum of TPE-B.

Conclusions

In this paper, a new type of molecule TPE-B has been designed based on the classic AIE molecule, and is used to construct a

fluorescent supramolecular polymer TPE-B@Q[10] through host-guest interactions. The system has the molar ratio of TPE-B:Q[10]:=1:2. Moreover, TPE-B@Q[10] overcomes the disadvantage of poor fluorescence performance of free TPE-B and has been successfully applied to the cell imaging of normal cells and HeLa cells. Flow cytometry further illustrated that Q[10] is capable of generating an alternative way to increase the fluorescence of TPE-B and its characteristic pattern for cellular imaging. Cytotoxicity experiments show TPE-B@Q[10] can be used for further in vivo studies, including drug delivery, drug tracking, organelle localization, *etc.* This work provides a theoretical basis for promoting the application of cucurbit[*n*]uril-based supramolecular polymers in biology, and will stimulate further development of cucurbit[*n*]uril chemistry.

Author Contributions

The manuscript was written through the contributions of all authors. All authors have approved the final version of the manuscript. ‡These authors contributed equally. (Match statement to author names with a symbol)

Conflicts of interest

There are no conflicts to declare.

Acknowledgments

This work was supported by the National Natural Science Foundation of China (No. 21861011, 21871064, 82060772) and the Innovation Program for High-level Talents of Guizhou Province (No. 2016-5657), The Graduate scientific research Fund of Guizhou Province (YJSKYJJ [2021] 021). CR thanks the EPSRC for an Overseas Travel Grant (EP/R023816/1).

Notes and references

[1] J. M. Lehn, Supramolecular Chemistry: Receptors, Catalysts, and Carriers, Science, 1985, 227, 849-856.
[2] C. J. Pedersen, The Discovery of Crown Ethers, Angew. Chem., Int. Ed. Engl., 1988, 27, 1021-1027.
[3] D. J. Cram, The Design of Molecular Hosts, Guests, and Their Complexes, Angew. Chem., Int. Ed. Engl., 1988, 27, 1009-1020.
[4] J. M. Lehn, Supramolecular Chemistry-Scope and Perspectives Molecules, Supermolecules, and Molecular Devices, Angew. Chem., Int. Ed. Engl., 1988, 27, 89-112.
[5] C. Fouquey, J. M. Lehn and A. M. Levelut, Molecular Recognition Directed Self-assembly of Supramolecular Liquid Crystalline Polymers from Complementary Chiral Components, Adv. Mater., 1990, 2, 254-257.
[6] L. Brunsveld, B. J. B. Folmer, E. W. Meijer and R. P. Sijbesma, Supramolecular Polymers, Chem. Rev. 2001, 101, 12, 4071-4098.
[7] T. Aida, E. W. Meijer and S. I. Stupp, Functional Supramolecular Polymers, Science, 2012, 335, 813-817.
[8] Chunju Li, Pillararene-based Supramolecular Polymers: from Molecular Recognition to Polymeric Aggregates, Chem. Commun., 2014, 50, 12420 -12433.
[9] W. A. Freeman, W. L. Mock, N. Y. Shih, Cucurbituril, J. Am. Chem. Soc. 1981, 103, 24, 7367-7368.
[10] Jae Wook Lee, S. Samal, N. Selvapalam, Hee-Joon Kim, and Kimoon Kim, Cucurbituril Homologues and Derivatives: New Opportunities in Supramolecular Chemistry, Acc. Chem. Res. 2003, 36, 8, 621-630.
[11] Simin Liu, Peter Y. Zavalij, and Lyle Isaacs, Cucurbit[10]uril, J. Am. Chem. Soc. 2005, 127, 48, 16798-16799.
[12] Xiran Yang, Fengbo Liu, Zhiyong Zhao, Feng Liang, Haijun Zhang, Simin Liu, Cucurbit[10]uril-based Chemistry, Chinese Chemical Letters, 2018, 29, 1560-1566.
[13] Guocan Yu, Kecheng Jie, and Feihe Huang, Supramolecular Amphiphiles Based on Host-Guest Molecular Recognition Motifs, Chem. Rev. 2015, 115, 15, 7240-7303.
[14] Xin-Long Ni, Shiyan Chen, Yaping Yang, and Zhu Tao, A Facile Cucurbit[8]uril-Based Supramolecular Approach to Fabricate Tunable Luminescent Materials in Aqueous Solution, J. Am. Chem. Soc. 2016, 138, 19, 6177-6183.
[15] Zhongzheng Gao, Jing Zhang, Nana Sun, Ying Huang, Zhu Tao, Xin Xiao and Jianzhuang Jiang, Hyperbranched Supramolecular Polymer Constructed from Twisted Cucurbit[14]uril and Porphyrin via Host-guest Interactions, Org. Chem. Front., 2016, 3, 1144-1148.
[16] Dan Yang, Ming Liu, Xin Xiao, Zhu Tao, Carl Redshaw, Polymeric Self-assembled Cucurbit[n]urils: Synthesis, Structures and Applications, Coordin. Chem. Rev., 2021, 434, 213733
[17] Henrique Dias Correia, Shagor Chowdhury, Ana Paula Ramos, Laure Guy, Grégoire Jean-François Demets and Christophe Bucher, Dynamic Supramolecular Polymers Built from Cucurbit[n]urils and Viologens, Polym Int 2019; 68: 572-588.
[18] Matthias Hartlieb, Edward D. H. Mansfield and Sebastien Perrier, A Guide to Supramolecular Polymerizations, Polym. Chem., 2020, 11, 1083-1110.
[19] Matthew J. Webber, Robert Langer, Drug delivery by supramolecular design, Chem. Soc. Rev., 2017,46, 6600-6620.
[20] Olga J. G. M. Goor, Simone I. S. Hendrikse Patricia Y. W. Dankers, E. W. Meijer, From supramolecular polymers to multi-component biomaterials, Chem. Soc. Rev., 2017,46, 6621-6637.
[21] Danyu Xia, Pi Wang, Xiaofan Ji, Niveen M. Khashab, Jonathan L. Sessler, Feihe Huang, Functional Supramolecular Polymeric Networks: The Marriage of Covalent Polymers and Macrocycle-Based Host-Guest Interactions, Chemical Reviews, 2020, 120, 13, 6070-612.
[22] Michelle J. Pisani, Yunjie Zhao, Lynne Wallace, Clifford E. Woodward, F. Richard Keene, Anthony I. Day, J. Grant Collins, Cucurbit[10]uril binding of dinuclear platinum(II) and ruthenium(II) complexes: association/dissociation rates from seconds to hours, Dalton Trans., 2010,39, 2078-2086.
[23] K. M. Anis-Ul-Haque, Clifford E. Woodward, Anthony I. Day, Lynne Wallace, Interaction of the Large Host Q[10] with Metal Polypyridyl Complexes: Binding Modes and Effects on Luminescence, Inorg. Chem. 2020, 59, 6, 3942-3953.
[24] Biyun Sun, Ian F. Musgrave, Anthony I. Day, Kirsten Heimann, F. Richard Keene, J. Grant Collins, Eukaryotic Cell Toxicity and HSA Binding of [Ru(Me4phen)(bb7)]2+ and the Effect of Encapsulation in Cucurbit[10]uril , Frontiers in Chemistry, 2018, 6, 595.
[25] Yang Yu, Yawen Li, Xiaoqing Wang, Hao Nian, Le Wang, Jie Li, Yanxia Zhao, Xiran Yang, Simin Liu, Liping Cao, Cucurbit[10] uril-Based [2]Rotaxane: Preparation and Supramolecular Assembly-Induced Fluorescence Enhancement, J. Org. Chem. 2017, 82, 11, 5590-5596.
[26] Hua Wang, Yuchong Yang, Bin Yuan, Xin-Long Ni, Jiang-Fei Xu, Xi Zhang, Cucurbit[10]uril-Encapsulated Cationic Porphyrins with Enhanced Fluorescence Emission and

Photostability for Cell Imaging, ACS Appl. Mater. Interfaces 2021, 13, 2269-2276
[27] J. D. Luo, Z. L. Xie, B. Z. Tang and et al., Aggregation-induced emission of 1-methyl-1,2,3,4,5-pentaphenylsilole, Chem. Commun., 2001, 1740-1741.
[28] Hong-Bo Cheng, Yuanyuan Li, Ben Zhong Tang and Juyoung Yoon, Assembly Strategies of Organic-based Imaging Agents for Fluorescence and Photoacoustic Bioimaging Applications, Chem. Soc. Rev., 2020, 49, 21-31.
[29] Frank Würthner, Aggregation-Induced Emission (AIE): A Historical Perspective, Angew. Chem. Int. Ed. 2020, 59,14192-14196.
[30] Tangxin Xiao, Jie Wang, Yong Shen, Cheng Bao, Zheng-Yi Li, Xiao-Qiang Sun, Leyong Wang, Preparation of A Fixed-tetraphenylethylene Motif Bridged Ditopic Benzo-21-crown-7 and Its Application for Constructing AIE Supramolecular Polymers, Chinese Chemical Letters, 2021, 32, 1377-1380.
[31] Zhao Li, Xiaofan Ji, Huilin Xie, and Ben Zhong Tang, Aggregation-Induced Emission-Active Gels: Fabrications, Functions, and Applications, Adv. Mater., 2021, 33, 2100021.
[32] Jie Li, Jianxing Wang, Haoxuan Li, Nan Song, Dong Wang and Ben Zhong Tang, Supramolecular materials based on AIE luminogens (AIEgens): construction and applications, Chem. Soc. Rev., 2020, 49, 1144-1172.
[33] Haotian Bai, Zhiyang Liu, Tianfu Zhang, Jian Du, Chengcheng Zhou, Wei He, Joe H. C. Chau, Ryan T. K. Kwok, Jacky W. Y. Lam, and Ben Zhong Tang, Multifunctional Supramolecular Assemblies with Aggregation-Induced Emission (AIE) for Cell Line Identification, Cell Contamination Evaluation, and Cancer Cell Discrimination, ACS Nano, 2020, 14, 6, 7552-7563.
[34] Liang Zhang, Tian-You Zhou, Jia Tian, Hui Wang, Dan-Wei Zhang, Xin Zhao, Yi Liu and Zhan-Ting Li, A Two-dimensional Single-layer Supramolecular Organic Framework That Is Driven by Viologen Radical Cation Dimerization and Further Promoted by Cucurbit[8]uril, Polym. Chem., 2014,5, 4715-4721.
[35] Zeyu Wang, Mingju Shui, Ian W. Wyman, Qing-Wen Zhang and Ruibing Wang, Cucurbit[8]uril-based Supramolecular Hydrogels for Biomedical Applications, RSC Med. Chem., 2021,12, 722-729.
[36] Ming Liu, Lixia Chen, Peihui Shan, Chengjie lian, Zenghui Zhang, Yunqian Zhang, Zhu Tao and Xin Xiao, Pyridine Detection Using Supramolecular Organic Frameworks Incorporating Cucurbit[10]uril, ACS Appl. Mater. Inter., 2021, 13, 7434−7442.
[37] Wei-Tao Xu, Yang Luo, Wei-Wei Zhao, Ming Liu, Guang-Yan Luo, Ying Fan, Rui-Lian Lin, Zhu Tao, Xin Xiao, Jing-Xin Liu, Detecting Pesticide Dodine by Displacement of Fluorescent Acridine from Cucurbit[10]uril Macrocycle, J. Agric. Food Chem., 2021, 69, 584-591.
[38] Fengbo Liu, Shagor Chowdhury, Roselyne Rosas, Valérie Monnier, Laurence Charles, Hakim Karoui, Didier Gigmes, Olivier Ouari, Floris Chevallier, Christophe Bucher, Anthony Kermagoret, Simin Liu, and David Bardelang, Triple Stack of a Viologen Derivative in a CB[10] Pair, Organic Letters 2021, 23, 14, 5283-5287.